

# Overexpression of FcγRIIB regulates downstream protein phosphorylation and suppresses B cell activation to ameliorate systemic lupus erythematosus

LINLIN SHENG<sup>1\*</sup>, XIUQIN CAO<sup>2\*</sup>, SHUHONG CHI<sup>1</sup>, JING WU<sup>1</sup>,  
HUIHUI XING<sup>1</sup>, HUIYU LIU<sup>1</sup> and ZHIWEI YANG<sup>1</sup>

<sup>1</sup>School of Basic Medical Sciences, <sup>2</sup>Key Laboratory of Fertility Preservation and Maintenance of Ministry of Education, Ningxia Medical University, Yinchuan, Ningxia 750004, P.R. China

Received November 24, 2019; Accepted July 14, 2020

DOI: 10.3892/ijmm.2020.4698

**Abstract.** The present study aimed to examine the effects of FcγRIIB on systemic lupus erythematosus (SLE) and to investigate the underlying mechanisms. For this purpose, lentiviral vector carrying the membrane-bound type FcγRIIB gene (mFcγRIIB lentivirus) and soluble FcγRIIB (sFcγRIIB) protein were used to treat B cells from patients with SLE. The B cells were treated with calf thymus DNA (ctDNA) and anti-calf thymus DNA-immune complexes (anti-ctDNA-IC). mFcγRIIB lentivirus and sFcγRIIB protein were also injected into MRL/lpr SLE mice. The results revealed that anti-ctDNA-IC treatment significantly downregulated the IgG antibody secretion of B cells treated with mFcγRIIB lentivirus. mFcγRIIB and sFcγRIIB decreased the phosphorylation level of Bruton's tyrosine kinase (BTK) in B cells, and increased the phosphorylation level of Lyn proto-oncogene (Lyn), docking protein 1 (DOK1) and inositol polyphosphate-5-phosphatase D (SHIP). mFcγRIIB promoted the apoptosis of B cells. Following the treatment of MRL/lpr SLE mice with mFcγRIIB lentivirus, the levels of urinary protein, serum anti-nuclear and

anti-dsDNA antibodies were decreased, while the levels of mFcγRIIB in B cells were increased. mFcγRIIB ameliorated the pathologies of the kidneys, liver and lymph node tissues of the MRL/lpr SLE mice. Following treatment of the MRL/lpr SLE mice with sFcγRIIB, the levels of urinary protein, serum anti-dsDNA antibody and BTK and SHIP phosphorylation levels in B cells were decreased, while the serum sFcγRIIB and sFcγRIIB-IgG levels were increased. On the whole, the findings of the present study demonstrate that recombinant FcγRIIB inhibits the secretion of IgG antibody by B cells from patients with SLE, ameliorates the symptoms of SLE in mice, and alters the phosphorylation levels of downstream proteins of the FcγRIIB signaling pathway in B cells. These results suggest that FcγRIIB may play preventive and therapeutic roles in SLE by inhibiting B cell activation via the FcγRIIB signaling pathway, which provides a novel theory and strategy for the prevention and treatment of SLE.

## Introduction

Systemic lupus erythematosus (SLE) is an autoimmune disease that affects several organs, including the skin, joints, central nervous system and kidneys. The occurrence of SLE is related to hormonal, environmental and genetic factors; however, the pathogenesis of SLE requires further study (1,2). High titers of autoantibodies against double-stranded DNA (dsDNA) and ribonucleoproteins (RNP) are often detectable in patients with SLE several years before clinical manifestations arise. These autoantibodies can bind to autoantigens and complement factors to form circulating immune complexes (CICs), which are deposited in target organs to induce inflammation and cause various diseases (3).

As the main force of the immune response, B cells play an important role in the humoral immune response. However, studies have demonstrated that B lymphocytes acting as effector cells can increase the occurrence and chronic persistence of SLE (4,5). Signal transduction abnormality, tolerance deficiency and immunoregulatory mechanism abnormality in B cells, induced by environmental and genetic factors, play important roles in the occurrence and development of SLE (6,7).

---

*Correspondence to:* Dr Zhiwei Yang, School of Basic Medical Sciences, Ningxia Medical University, 1160 Shengli Street, Xingqing, Yinchuan, Ningxia 750004, P.R. China  
E-mail: yangzhw0817@163.com

\*Contributed equally

**Abbreviations:** SLE, systemic lupus erythematosus; dsDNA, double-stranded DNA; RNP, ribonucleoproteins; CICs, circulating immune complexes; ctDNA, calf thymus DNA; ICs, immune complexes; mFcγRIIB, membrane-bound type FcγRIIB; sFcγRIIB, soluble FcγRIIB; BTK, Bruton's tyrosine kinase; Lyn, Lyn proto-oncogene, Src family tyrosine kinase; DOK1, docking protein 1; SHIP, inositol polyphosphate-5-phosphatase D; BCR, B cell receptor

**Key words:** FcγRIIB, B cells, systemic lupus erythematosus, IgG antibody, Bruton's tyrosine kinase, Lyn, docking protein 1, inositol polyphosphate-5-phosphatase D

Fc $\gamma$ RIIB, as an immunoregulatory receptor, is expressed mainly on the surface of B cells. It contains the extracellular region with the Ig-like domain, transmembrane region and intracellular region with the immunoreceptor tyrosine inhibitory motif (ITIM), which has an inhibitory function. The extracellular domain is a low affinity binding IgG-Fc region. Antigens and cytokines can stimulate the hydrolysis of the extracellular domain of membrane-bound type Fc $\gamma$ RIIB (mFc $\gamma$ RIIB) or the selective splicing of the Fc $\gamma$ RIIB gene to produce soluble Fc $\gamma$ RIIB (sFc $\gamma$ RIIB) (8). Fc $\gamma$ RIIB can regulate healthy B cells, induces immune tolerance by inhibiting B cell expression of antibodies, and is a key inhibitory receptor mediating B cells activation (9,10). The inhibitory effect of Fc $\gamma$ RIIB depends on the ITIM that is phosphorylated upon Fc $\gamma$ RIIB coaggregation with ITAM-bearing receptors and recruits SH2 domain-containing phosphatases (11). The decrease in Fc $\gamma$ RIIB expression exerts adverse effects on the immune response, leading to the occurrence of autoimmune diseases. The level of Fc $\gamma$ RIIB on the surfaces of immature B cells and memory B cells in patients with autoimmune diseases has been found to be lower than that in healthy subjects (12,13), causing B lymphocytes to produce a large number of antibodies against autoantigens in a hyperimmune response. However, it has been reported that increasing the expression of Fc $\gamma$ RIIB in B lymphocytes reduces the production of antibodies and immune complexes in lupus mice, and improves the symptoms of lupus (14). In transgenic mice with Fc $\gamma$ RIIB overexpression on the surface of B lymphocytes, the production of T cell-dependent antibody IgG has been shown to be significantly reduced, and the symptoms of SLE are decreased (15). Therefore, increasing the Fc $\gamma$ RIIB levels on the surface of B cells may be a promising approach for treating autoimmune diseases. Recombinant human sFc $\gamma$ RIIB can be used as a potential target for the treatment of autoimmune diseases mediated by antibodies and immune complexes. However, to the best of our knowledge, there are no available reports to date on the negative regulation of antibody secretion in patients with SLE by recombinant human sFc $\gamma$ RIIB. More importantly, the mechanisms of Fc $\gamma$ RIIB in SLE remain unclear. In the present study, the effects of mFc $\gamma$ RIIB and sFc $\gamma$ RIIB proteins on the IgG antibody secretion of B cells from patients with SLE, and the preventative and therapeutic effects of sFc $\gamma$ RIIB in mice with SLE were examined. In addition, the underlying mechanisms were investigated by measuring the phosphorylation levels of Bruton's tyrosine kinase (BTK), DOK1, docking protein 1 (DOK1), Lyn proto-oncogene (Lyn) and inositol polyphosphate-5-phosphatase D (SHIP) in the downstream signaling pathways of B cell receptor (BCR) and Fc $\gamma$ RIIB in B cells.

## Materials and methods

**Construction of mFc $\gamma$ RIIB lentivirus.** Total RNA from was isolated human B cells (isolated from patients with SLE as described below) using TRIzol RNA extraction reagent (Invitrogen; Thermo Fisher Scientific, Inc.). Subsequently, cDNA was synthesized using 1  $\mu$ g of total RNA and the reverse transcription system [Tiangen Biochemical Technology (Beijing) Co., Ltd.]. The Fc $\gamma$ RIIB gene was cloned by nest PCR using Taq PCR MasterMix [Tiangen Biochemical

Technology (Beijing) Co., Ltd.] and outer primers (forward primer, 5'-ATCCGCCAAGCTTTGAGAGAAGGCTGTGAC T-3' and reverse primer, 5'-AGGGAGCTTCAGGACTCAGGTAGATGACT-3') at 58°C annealing temperature for the first PCR and inner primers (forward primer, 5'-GCCCCGGGACGCGTATGGGAATCCTGTCAATCTTACC-3' and reverse primer, 5'-CTACCCGGTAGAATTCCTAAATACGGTTCTGGTCATCAG-3') at 56°C annealing temperature for the second PCR. The Fc $\gamma$ RIIB gene was inserted into the lentivirus-induced expression vector pLVX-TRE3G-ZsGreen1 (Takara Bio, Inc.) with green fluorescent protein (GFP) gene to construct the mFc $\gamma$ RIIB lentivirus.

**Lentivirus packaging.** The constructed human mFc $\gamma$ RIIB lentivirus ( $10^6$  TU/ml), mouse mFc $\gamma$ RIIB lentivirus ( $10^6$  TU/ml) from our laboratory, and virus tetracycline (Tet) ( $10^5$  TU/ml) regulatory plasmid were transfected into lenti-X 293T cells (Takara Bio, Inc.) to complete lentivirus packaging using a Lenti-X Lentiviral packaging system (Takara Bio, Inc.), according to the manufacturer's instructions.

**HT-1080 cell culture.** HT-1080 cells were purchased from the Shanghai Institutes for Biological Sciences, and were cultured in Dulbecco's modified Eagle's medium (HyClone; GE Healthcare Life Sciences) supplemented with 10% (v/v) fetal bovine serum (HyClone; GE Healthcare Life Sciences) and penicillin-streptomycin (Invitrogen; Thermo Fisher Scientific, Inc.) in a 95% O<sub>2</sub> and 5% CO<sub>2</sub> incubator at 37°C.

**Establishment of HT-1080 cells stably expressing mFc $\gamma$ RIIB.** A total of  $2 \times 10^5$  HT-1080 cells were infected with lentivirus regulatory plasmid, followed by the addition of 1 ml of polyethylene (10 mg/ml) virus diluent (diluted 6 times) to HT-1080 cells for infection, incubate at 37°C, 5% CO<sub>2</sub> for 12 h, and then add G418 (100  $\mu$ g/ $\mu$ l) or Puro (0.3  $\mu$ g/ $\mu$ l) working solution, G418 (200  $\mu$ g/ml) was used to screen single G418-resistant HT-1080 cells. Subsequently, scale-up cultured G418-resistant HT-1080 cells were infected with mFc $\gamma$ RIIB lentivirus, and single G418- and Puro-resistant HT-1080 cells were then screened using Puro (0.3  $\mu$ g/ml, Takara Bio, Inc.), cultured at 37°C, 5% CO<sub>2</sub> for 7-14 days; the viral titer was  $4 \times 10^7$  TU/ml.

**Immunofluorescence assay.** G418- and Puro-resistant HT-1080 cells were inoculated into 6-well plates, and inducer doxycycline (Dox) (Takara Bio, Inc.) was added to induce the cells at a final concentration of 1,000 ng/ml. The cells were then incubated for 48 h at 37°C with 5%CO<sub>2</sub>. After washing with PBS, PE-labeled anti-Fc $\gamma$ RIIB antibody (cat. no. 563019; 5  $\mu$ l; BD Biosciences) was incubated with the cells for 20 min on ice and in the dark. After washing with PBS, cells were observed under transmission light, green fluorescence and red fluorescence microscopes (Olympus Corporation).

**Western blot analysis.** Double-resistant HT-1080 cells were induced by Dox inducer at concentrations of 100, 500, 1,000 ng/ml and incubated for 48 h at 37°C with 5% CO<sub>2</sub>. Total protein was extracted from the cells using lysis buffer (KeyGEN BioTECH). After determining the protein concentration using the BCA analysis kit (KeyGEN BioTECH), an equal amount of proteins (100 ng) were separated by 10%

SDS-PAGE, and then transferred to polyvinylidene difluoride membranes, which were blocked with 5% skim milk in TBS with 1% Tween-20 for 90 min at 25°C. Subsequently, the membranes were probed with primary antibodies at 4°C overnight, followed by incubation with secondary antibodies for a further 2 h at room temperature, each sample of total protein was assayed by western blot analysis using mouse monoclonal anti-human Fc $\gamma$ RIIB antibody (cat. no. sc-166711; 1:2,000; Santa Cruz Biotechnology, Inc.) and peroxidase-conjugated rabbit anti-mouse IgG antibody (cat. no. sc-2357; 1:2,000; Santa Cruz Biotechnology, Inc.) (16). The immunoreactive bands were visualized using an enhanced chemiluminescent (ECL) kit (KeyGEN BioTECH). The blots were analyzed using ImageJ 1.48u software (National Institutes of Health).  $\beta$ -actin (cat. no. sc-81178; 1:500; Santa Cruz Biotechnology, Inc.) was used as the loading control.

**Preparation of recombinant sFc $\gamma$ RIIB.** In order to prepare human recombinant sFc $\gamma$ RIIB, PET-sFc $\gamma$ RIIB plasmid from our laboratory was transformed into competent *Escherichia coli* BL21 cells (Takara Bio, Inc.). To prepare mouse recombinant sFc $\gamma$ RIIB, mouse sFc $\gamma$ RIIB gene was cloned using TRE-sFc $\gamma$ RIIB plasmid as a template and sFc $\gamma$ RIIB primers (forward primer, 5'-GGAATTCATGGGAATCCTGCCGTT CCTACTGA-3' and reverse primer, 5'-CCCAAGCTTTGT CAATACTGGTAAAGACCTGCTG-3'), and was inserted into pET-32a (+) (Beijing Solarbio Science & Technology Co., Ltd.) vector to construct the PET-sFc $\gamma$ RIIB plasmid. The PET-sFc $\gamma$ RIIB plasmid (2  $\mu$ l) was subsequently transformed into competent *Escherichia coli* BL21 cells. Both sets of transformed BL21 cells were induced by IPTG to produce sFc $\gamma$ RIIB proteins, which were purified using a His Bind<sup>®</sup> Purification kit (Merck & Co., Inc.) according to the manufacturer's instructions. Purified sFc $\gamma$ RIIB proteins were validated by western blot analysis.

**ELISA for sFc $\gamma$ RIIB and IgG.** A total of 30 female patients with SLE (35 $\pm$ 10 years old) from the Department of Rheumatism, General Hospital of Ningxia Medical University were recruited into the present study based on the American College of Rheumatology (ACR) criteria (17), and 30 healthy female subjects (37 $\pm$ 8 years old) from the Cardiovascular Hospital of Ningxia Medical University were also recruited (October, 2018 to March, 2019). All subjects signed informed consent forms prior to the start of the study. The present study was approved by the Ethics Committee of Ningxia Medical University. Serum was collected from all subjects. For serum sFc $\gamma$ RIIB detection, mouse anti-human sFc $\gamma$ RIIB monoclonal antibody (cat. no. sc-166578; 1:2,000; Santa Cruz Biotechnology, Inc.), serum (1:100; Biological Industries), rabbit anti-human sFc $\gamma$ RIIB polyclonal antibody (cat. no. bs-4991R; 1:2,000; Beijing Bioss Biotechnology Co., Ltd.) and HRP-labeled anti-IgG (cat. no. bs-0297G-HRP; 1:8,000; Beijing Bioss Biotechnology Co., Ltd.) were successively added into the plates for incubation (37°C, 30 min). For serum sFc $\gamma$ RIIB-IgG determination, mouse anti-human sFc $\gamma$ RIIB monoclonal antibody (cat. no. bs-4991R; 1:2,000; Beijing Bioss Biotechnology Co., Ltd.), serum (1:100; Biological Industries), and HRP-labeled anti-IgG (cat. no. bs-0297G-HRP; 1:8,000; Beijing Bioss Biotechnology Co., Ltd.) were successively incubated in plates

(37°C, 30 min). For the binding strength detection of recombinant human sFc $\gamma$ RIIB to IC in serum, serum treated with 5  $\mu$ g/ml calf thymus DNA (ctDNA; Sigma-Aldrich; Merck KGaA) and HRP-labeled anti-IgG (cat. no. bs-40295G-HRP; 1:8,000; Beijing Bioss Biotechnology Co., Ltd.) were successively incubated (37°C, 30 min) in plates previously coated with 1.25  $\mu$ g/ml recombinant sFc $\gamma$ RIIB. Following these incubations, TMB reagent was added to all plates for chromogenic reaction. The optical density was determined using a microplate reader (ELx800NB, BioTek Instruments, Inc.).

**B cell preparation.** Peripheral blood samples were collected from all study participants and the lymphocytes were isolated with lymphocyte separation liquid. A magnetic bead separation system (Miltenyi Biotec GmbH) was used to sort CD19<sup>+</sup> B cells with anti-CD19<sup>+</sup> antibody (cat. no. 130-113-733; 1:50; Miltenyi Biotec GmbH). Sorted CD19<sup>+</sup> B cells were cultured for scale-up.

**B cell treatment.** For mFc $\gamma$ RIIB treatment, mFc $\gamma$ RIIB lentivirus, lentivirus regulatory plasmid and Dox were added to the CD19<sup>+</sup> B cells. The expression of mFc $\gamma$ RIIB in the treated B cells was then detected by immunofluorescence assay and western blot analysis according to the procedures described above. Subsequently, ctDNA and anti-ctDNA-IC (the mixture of SLE patient serum and ctDNA at a final concentration of 5  $\mu$ g/ml, incubated at 37°C for 1 h) were incubated with treated CD19<sup>+</sup> B cells. After 24 h, the B cells were collected for flow cytometry. Briefly, the collected cells were washed twice with ice-cold PBS at pH 7.4, and were then resuspended in buffer containing Annexin V (Elabscience); at a concentration of 1 $\times$ 10<sup>6</sup>/ml cells/ml. Subsequently, 5  $\mu$ l Alexa Fluor 555 (Thermo Fisher Scientific, Inc.) and 1  $\mu$ l 100  $\mu$ g/ml PI (Thermo Fisher Scientific, Inc.) were added to 100  $\mu$ l cell suspension. After gentle vortexing, the cells were incubated at 4°C in the dark for 15 min and analyzed by flow cytometry (Merck KGaA). The percentages of positively stained cells were determined. For sFc $\gamma$ RIIB treatment, recombinant sFc $\gamma$ RIIB and ctDNA were used to treat CD19<sup>+</sup> B cells for 72 h. Cell medium from both virus and protein treatments was collected for IgG detection using an ELISA kit (eBioscience), according to the manufacturer's instructions. B cells were collected for the determination of the BTK, Lyn, DOK1 and SHIP protein and phosphorylation levels by western blot analysis using antibodies against BTK (cat. no. ab208937; 1:500; Abcam), Lyn (cat. no. ab1890; 1:1,000; Abcam), DOK1 (cat. no. ab8112; 1:1,000; Abcam), SHIP (cat. no. ab45142; 1:1,000; Abcam), phosphorylated BTK (cat. no. ab68217; 1:1,000; Abcam), phosphorylated DOK1 (cat. no. ab75742; 1:1,000; Abcam), phosphorylated Lyn (cat. no. ab33914; 1:1,000; Abcam) and phosphorylated SHIP (cat. no. ab96402; 1:1,000; Abcam), the membranes were probed with primary antibodies at 4°C overnight, followed by incubation with secondary antibodies for a further 2 h at room temperature.

**Animal experiments.** A total of 160 MRL/lpr SLE model mice (all female mice) with a body weight of 16-20 g were purchased from the Experimental Animal Center of Nanjing Military Region (no. 0032260). All animals were kept in cages with a light/dark cycle of 12 h at 25 $\pm$ 1°C, with free access

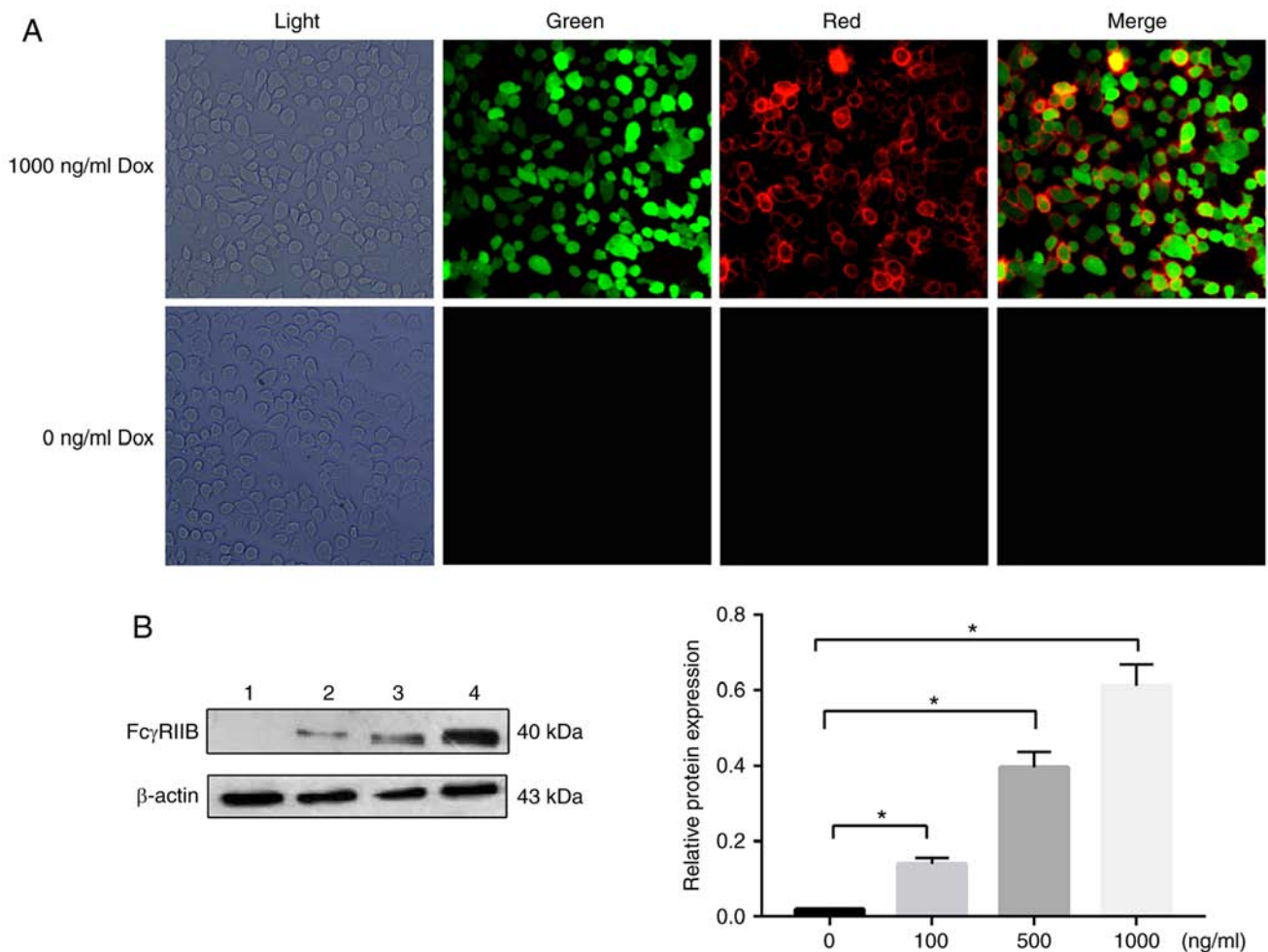


Figure 1. (A) Observation of double-resistant HT-1080 cells by fluorescence microscopy (magnification  $\times 400$ ). The expression of human mFc $\gamma$ RIIB in HT-1080 cells was detected by immunofluorescence staining. Light, light field; green, green fluorescent protein (GFP) expression in cells; red, mFc $\gamma$ RIIB expression in cells; merge, GFP and mFc $\gamma$ RIIB expression in cells. The experiments were repeated 3 times. (B) The protein expression levels of sFc $\gamma$ RIIB in human were examined by western blot analysis, with  $\beta$ -actin as a loading control. Lane 1, 0 ng/ml Dox inducer; lane 2, 100 ng/ml Dox inducer; lane 3, 500 ng/ml Dox inducer; lane 4, 1,000 ng/ml Dox inducer. \* $P < 0.05$ . Data are presented as the means  $\pm$  SD of 3 independent experiments. Dox, doxycycline; mFc $\gamma$ RIIB, membrane-bound type Fc $\gamma$ RIIB; sFc $\gamma$ RIIB, soluble Fc $\gamma$ RIIB.

to food and water; the health and behavior of the mice were monitored every 5 days. Among the 160 mice, mice (8 weeks old) that had no lupus symptoms were designated as the prevention group ( $n=80/\text{group}$ ) and 16-week-old mice that had obvious lupus symptoms were designated as the treatment group ( $n=80/\text{group}$ ). The animal experiments were approved by the Animal Ethics Committee of Ningxia Medical University and followed the Guidelines for the Management and Use of Laboratory Animals (National Academies Press). For mFc $\gamma$ RIIB treatment, the prevention (pre) and treatment (tre) groups were treated with 100  $\mu\text{l}$  or 200  $\mu\text{l}$  suspensions of mFc $\gamma$ RIIB lentivirus, lentivirus regulatory plasmid and Dox, 100  $\mu\text{l}$  suspensions of lentivirus empty vector, and healthy saline via the tail vein ( $n=10/\text{group}$ ). For sFc $\gamma$ RIIB treatment, the prevention group and treatment groups were treated with intravenous 4.8  $\mu\text{g}$  (60  $\mu\text{l}$ ), 9.6  $\mu\text{g}$  (120  $\mu\text{l}$ ), and 14.4  $\mu\text{g}$  (180  $\mu\text{l}$ ) recombinant mouse Fc $\gamma$ RIIB and normal saline, once per week for 4 consecutive weeks ( $n=10/\text{group}$ ). Following observation for a week, serum and urine were collected, and the mice were then anesthetized by an intraperitoneal injection of chloral hydrate (4%, 400 mg/kg) and were sacrificed by cervical

dislocation. Mouse death was confirmed by the inexistence of breath, heartbeat and corneal reflex. No accidental deaths occurred during the experiment.

Kidney, liver and lymph tissues were obtained for H&E staining. The mice were sacrificed and the kidney, liver and lymph tissues of the mice were obtained and fixed in 4% (v/v) paraformaldehyde, embedded in paraffin and sectioned at a 5–8  $\mu\text{m}$  thickness. The fixed kidney, liver and lymph tissues were stained with hematoxylin and eosin (H&E) for the evaluation of the severity of kidney, liver and lymph injury. The samples were dewaxed with xylene (cat. no. 10023428; Sinopharm Chemical Reagent Co., Ltd.) and then dephenylated using a graded ethanol series (100, 95, 80 and 70%) for 2 min. The tissues were then rehydrated by rinsed in distilled water twice to, stained using 0.5% hematoxylin (cat. no. G1120; Solarbio Life Science Co., Ltd.) for 20 min at room temperature and then washed under running water. The slices were then rinsed in acidification solution comprised of hydrochloric acid (cat. no. 10011018; Sinopharm Chemical Reagent Co., Ltd.) and 75% ethanol for 30 sec and then washed with tap water for 15 min. The tissues were then stained using

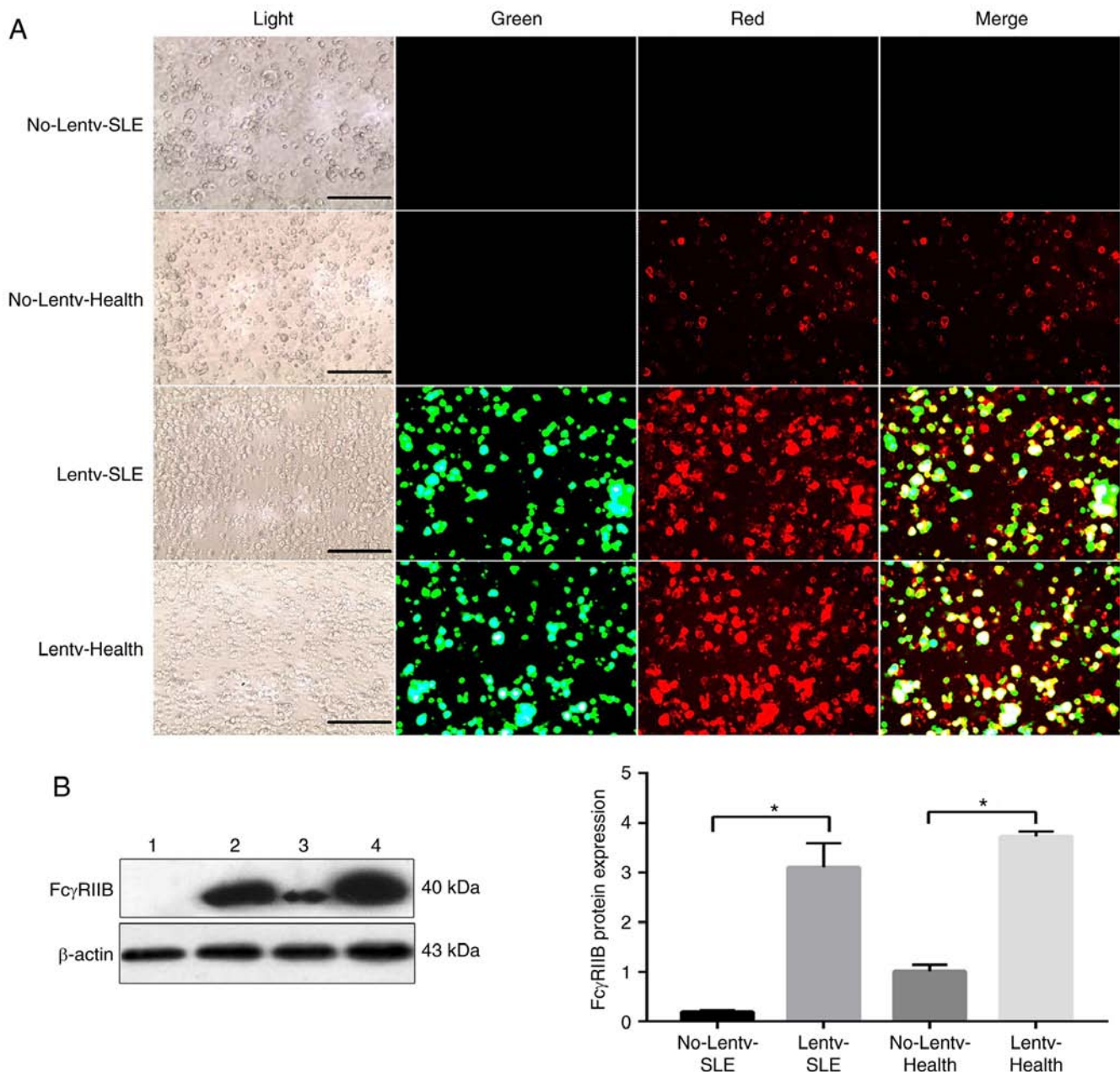


Figure 2. (A) Fluorescence microscopy to observe the expression of mFc $\gamma$ RIIB in B lymphocytes (magnification 400x). B cells were transfected using mFc $\gamma$ RIIB-lentivirus for 72 h. The infection efficiency of mFc $\gamma$ RIIB-lentivirus was observed by fluorescence microscopy. No-Lentv-SLE, no transfection in the SLE patients; Lentv-SLE, mFc $\gamma$ RIIB-lentivirus transfection in the SLE patients; No-Lentv-health, no transfection in the healthy controls; Lentv-health, mFc $\gamma$ RIIB-lentivirus transfection in the healthy controls. Light, light field; green, green fluorescent protein (GFP) expression in cells; red, mFc $\gamma$ RIIB expression in cells; merge, GFP and mFc $\gamma$ RIIB expression in cells. The experiments were repeated 3 times. (B) The protein expression levels of mFc $\gamma$ RIIB in human were examined by western blot analysis, with  $\beta$ -actin as a loading control. Lane 1, Control SLE group; lane 2, virus-infected SLE group; lane 3, healthy control group; lane 4, virus-infected healthy group. \*P<0.05. Data are presented as the means  $\pm$  SD of 3 independent experiments. mFc $\gamma$ RIIB, membrane-bound type Fc $\gamma$ RIIB; sFc $\gamma$ RIIB, soluble Fc $\gamma$ RIIB.

0.5% eosin (cat. no. G1120; Solarbio Life Science Co., Ltd.) for 2 min at room temperature, dehydrated in 100% ethanol for 1 min and treated with xylene for 3 min. Finally, neutral gum was used to seal the film.

The urine albumin (mouse albumin ELISA kit; cat. no. AKRAL-121; Shibayagi), serum anti-dsDNA antibody [mouse anti-double stranded DNA antibody (IgG) ELISA kit; cat. no. CSB-E11194m; Cusabio] and serum anti-nuclear antibody [mouse anti-nuclear antibody (IgM) ELISA kit; cat. no. 88-50470-22; eBioscience] were detected according to the manufacturer's instructions. Serum-free Fc $\gamma$ RIIB was

measured using rabbit anti-mouse Fc $\gamma$ RIIB monoclonal antibody (cat. no. sc-166711; 1:2,000, Santa Cruz Biotechnology, Inc.) and goat anti-mouse Fc $\gamma$ RIIB polyclonal antibody (cat. no. sc-12815; 1:2,000; Santa Cruz Biotechnology, Inc.). Serum Fc $\gamma$ RIIB-IgG was assayed using rabbit anti-mouse Fc $\gamma$ RIIB monoclonal antibody (cat. no. sc-365864; 1:2,000; Santa Cruz Biotechnology, Inc.) and HRP-labeled goat anti-mouse IgG antibody (cat. no. bs-0296G-HRP; 1:5,000; Beijing Bioss Biotechnology Co., Ltd.). Lymphocytes were isolated from spleens using lymphocyte separation solution (Tianjin Hao Yang Hua Ke Co., Ltd.). B cells were sorted using

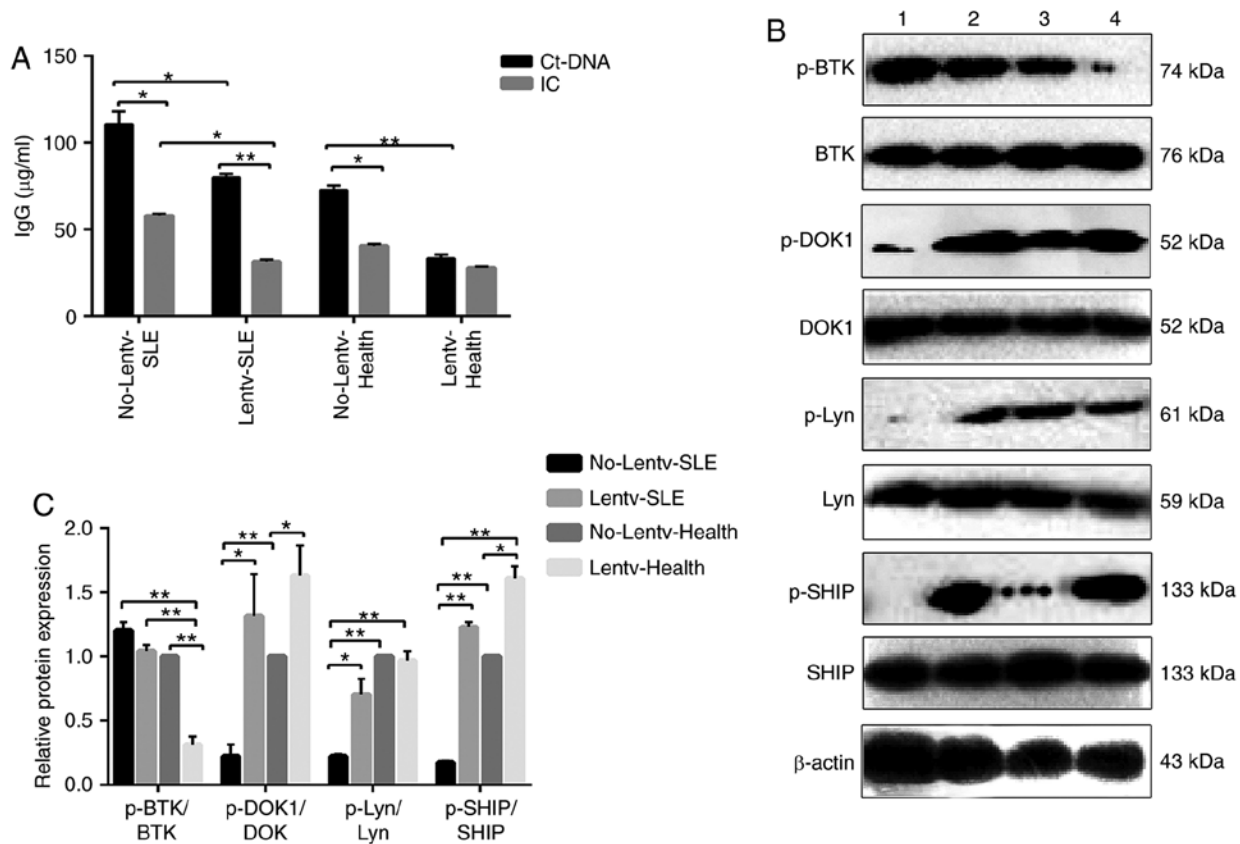


Figure 3. (A) ELISA detection of human IgG antibody levels. No-Lentv-SLE, control SLE group; Lentv-SLE, virus-infected SLE group; No-Lentv-Health, healthy control group; Lentv-Health, virus-infected healthy group; CtDNA, calf thymus DNA. IC, anti-calf thymus DNA-immune complexes. \* $P < 0.05$ ; \*\* $P < 0.01$ . The experiments were repeated 3 times. (B and C) The human protein expression levels of BTK, p-BTK, DOK1, p-DOK1, Lyn, p-Lyn, SHIP and p-SHIP were examined by western blot analysis, with  $\beta$ -actin as a loading control. The phosphorylation and total protein levels of BTK, DOK1, Lyn and SHIP were detected in B cells from patients with SLE and healthy subjects infected with mFc $\gamma$ RIIB lentivirus following anti-ctDNA-IC stimulation, and the relative level for each phosphorylation-protein/each respective total protein was calculated. No-Lentv-SLE, control SLE group; Lentv-SLE, virus-infected SLE group; No-Lentv-Health, healthy control group; Lentv-Health, virus-infected healthy group. \* $P < 0.05$ ; \*\* $P < 0.01$ . Data are presented as the means  $\pm$  SD of 3 independent experiments. SLE, systemic lupus erythematosus; mFc $\gamma$ RIIB, membrane-bound type Fc $\gamma$ RIIB; sFc $\gamma$ RIIB, soluble Fc $\gamma$ RIIB; BTK, Bruton's tyrosine kinase; Lyn, Lyn proto-oncogene, Src family tyrosine kinase; DOK-1, docking protein 1; SHIP, inositol polyphosphate-5-phosphatase D.

mouse anti-CD19 microbeads (Miltenyi Biotec GmbH). The protein and phosphorylation levels of BTK, Lyn and SHIP in the B cells were detected by western blot analysis using BTK polyclonal antibody (cat. no. 21581-1-AP; 1:1,000; Proteintech), phospho-BTK antibody (cat. no. 5082T; 1:1,000; Cell Signaling Technology, Inc.), Lyn polyclonal antibody (cat. no. BS6657; 1:1,000; Bioworld), phospho-Lyn (cat. no. BS64043; 1:500; Bioworld), SHIP polyclonal antibody (cat. no. BS91238; 1:1,000; Bioworld), phospho-SHIP (cat. no. BS94059; 1:1,000; Bioworld).

**Statistical analysis.** Statistical analyses were performed using SPSS 23.0 (IBM Corp.) and the results are presented as the means  $\pm$  standard error of mean (SEM). When the data exhibited a normal distribution, one-way analysis of variance (ANOVA) with Tukey's post hoc test were used for multiple comparisons, and the SNK-q test was used for the comparison between 2 groups. When the data exhibited a non-normal distribution, the Kruskal-Wallis test (Mann-Whitney U with Bonferroni's correction applied) was used. Statistically significant values were indicated by  $P < 0.05$ . Graph construction was performed using GraphPad Prism software version 5 (GraphPad Software).

## Results

**Successful construction of mFc $\gamma$ RIIB lentivirus and mFc $\gamma$ RIIB expression in HT-1080 cells.** The human TRE-mFc $\gamma$ RIIB lentiviral vector was successfully constructed with the sequencing results indicating that the inserted mFc $\gamma$ RIIB gene was 100% homologous to that provided by GenBank. The lentiviral vector titer was  $10^6$  TU/ml and the lentiviral regulatory plasmid titer was  $10^5$  TU/ml and exhibited good infectivity (data not shown). After infecting the HT-1080 cells with the virus, mFc $\gamma$ RIIB expression was induced with 1,000 ng/ml Dox. Immunofluorescence staining revealed that mFc $\gamma$ RIIB lentivirus successfully infected HT-1080 cells indicated by the green fluorescence emitted by expressed GFP, and mFc $\gamma$ RIIB was expressed in the cytomembrane of the HT-1080 cells indicated by red fluorescence (Fig. 1A). Western blot assays revealed that the mFc $\gamma$ RIIB expression level was positively associated with the inducer concentration, as shown in Fig. 1B.

**Expression of mFc $\gamma$ RIIB in human B cells.** Similarly, as shown in Fig. 2A, green fluorescence indicated that the mFc $\gamma$ RIIB lentivirus was successfully infected into B cells, and red fluorescence indicated that mFc $\gamma$ RIIB was expressed

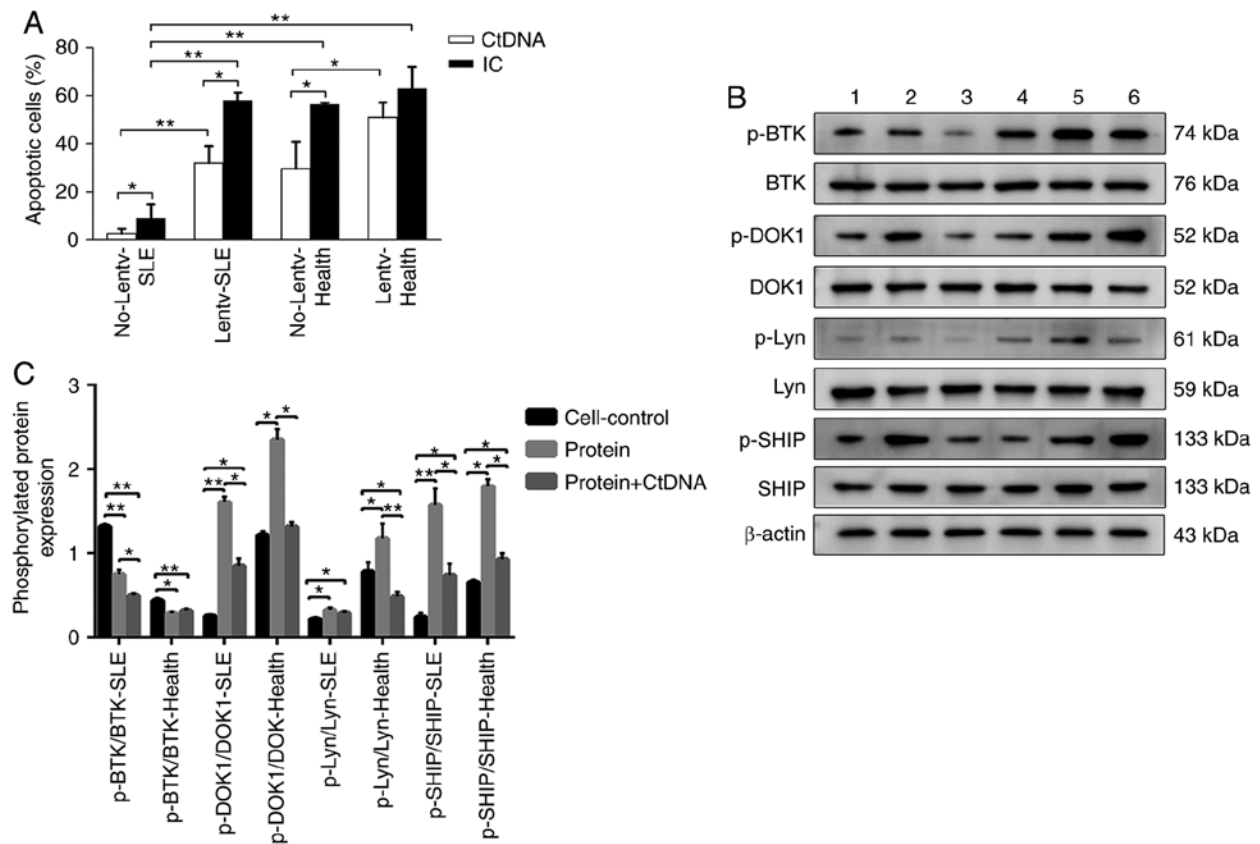


Figure 4. (A) Apoptotic rate of B cells infected by human mFc $\gamma$ RIIB lentivirus. No-Lentv-SLE, control SLE group; Lentv-SLE, virus-infected SLE group; No-Lentv-Health, healthy control group; Lentv-Health, virus-infected healthy group; CtDNA, calf thymus DNA; IC, anti-calf thymus DNA-immune complexes. \* $P$ <0.05; \*\* $P$ <0.01. The experiments were repeated 3 times. (B and C) The human protein expression levels of BTK, p-BTK, DOK1, p-DOK-1, Lyn, p-Lyn, SHIP and p-SHIP were examined by western blot analysis, with  $\beta$ -actin as a loading control. The phosphorylation and total protein levels of BTK, DOK-1, Lyn and SHIP were detected in B cells of patients with SLE and healthy subjects following treatment with human sFc $\gamma$ RIIB or sFc $\gamma$ RIIB plus ctDNA, and the relative level for each phosphorylation-protein/each respective total protein was calculated. Cell-Control-SLE, B cells of SLE patients; Protein-SLE, B cells of SLE patients treated with sFc $\gamma$ RIIB; Protein + CtDNA-SLE, B cells of SLE patients treated with sFc $\gamma$ RIIB and ctDNA; Cell-Control-Health, B cells of healthy subjects; Protein-Health, B cells of healthy persons treated with sFc $\gamma$ RIIB; Protein + CtDNA-Health, B cells of healthy persons treated with sFc $\gamma$ RIIB and ctDNA. \* $P$ <0.05; \*\* $P$ <0.01. Data are presented as the means  $\pm$  SD of 3 independent experiments. SLE, systemic lupus erythematosus; mFc $\gamma$ RIIB, membrane-bound type Fc $\gamma$ RIIB; sFc $\gamma$ RIIB, soluble Fc $\gamma$ RIIB; BTK, Bruton's tyrosine kinase; Lyn, Lyn proto-oncogene, Src family tyrosine kinase; DOK-1, docking protein 1; SHIP, inositol polyphosphate-5-phosphatase D.

Table I. Total sFc $\gamma$ RIIB and sFc $\gamma$ RIIB-IgG levels in human serum (n=30, ng/ml, means  $\pm$  SD).

Group	Content
SLE total sFc $\gamma$ RIIB	125.11 $\pm$ 4.63 <sup>a</sup>
Health total sFc $\gamma$ RIIB	134.30 $\pm$ 5.89
SLE sFc $\gamma$ RIIB-IgG	89.23 $\pm$ 13.07 <sup>b</sup>
Health sFc $\gamma$ RIIB-IgG	132.64 $\pm$ 6.20

<sup>a</sup> $P$ <0.05 vs. healthy total sFc $\gamma$ RIIB; <sup>b</sup> $P$ <0.01 vs. healthy sFc $\gamma$ RIIB-IgG. SLE, systemic lupus erythematosus; mFc $\gamma$ RIIB, membrane-bound type Fc $\gamma$ RIIB; sFc $\gamma$ RIIB, soluble Fc $\gamma$ RIIB.

in the cytomembrane of B cells. In addition, immunofluorescence staining (Fig. 2A) and western blot analysis (Fig. 2B) revealed that the expression level of endogenous mFc $\gamma$ RIIB in the B cells of patients with SLE was lower than that in the healthy controls. mFc $\gamma$ RIIB expression in the virus-infected SLE group was significantly higher than that in the control

SLE group. Similarly, the expression of mFc $\gamma$ RIIB in the virus-infected healthy group was higher than that in the control healthy group.

*Effects of overexpression of mFc $\gamma$ RIIB on human B cells.* ctDNA and anti-ctDNA-IC were used to stimulate infected B cells. ELISA was performed to detect anti-IgG antibody secreted by B cells, and the protein and phosphorylation levels of BTK, Lyn, DOK1 and SHIP were detected by western blot analysis. The results revealed that the IgG levels in the virus-infected SLE and healthy groups were respectively significantly lower than those in the control SLE and control healthy groups. Anti-ctDNA-IC treatment significantly downregulated the B cell secretion of IgG antibody, apart from the virus-infected healthy group (Fig. 3A). The relative expression levels of p-DOK1/DOK1, p-SHIP/SHIP in the virus-infected SLE and virus-infected healthy groups were respectively significantly higher than those in the control SLE and control healthy groups; the relative expression levels of p-Lyn/Lyn in the virus-infected SLE, virus-infected healthy groups and control healthy groups were respectively significantly higher than those in the control SLE

Table II. Soluble Fc $\gamma$ RIIB binding to immune complexes, with OD values (n=30, means  $\pm$  SD).

Group DNA (mg/ml)	OD value						
	0	0.05	0.1	0.2	0.4	0.8	1.0
SLE	1.239 $\pm$ 0.061 <sup>a</sup>	1.439 $\pm$ 0.065 <sup>a</sup>	1.507 $\pm$ 0.065 <sup>a</sup>	1.569 $\pm$ 0.068 <sup>a</sup>	1.653 $\pm$ 0.075 <sup>a</sup>	1.763 $\pm$ 0.068 <sup>a</sup>	1.776 $\pm$ 0.065 <sup>a</sup>
Healthy	1.776 $\pm$ 0.065	1.258 $\pm$ 0.054	1.323 $\pm$ 0.063	1.394 $\pm$ 0.065	1.464 $\pm$ 0.072	1.546 $\pm$ 0.072	1.557 $\pm$ 0.067
PBS	0.097	0.076	0.083	0.086	0.091	0.072	0.095

<sup>a</sup>P<0.05 vs. healthy group. SLE, systemic lupus erythematosus; sFc $\gamma$ RIIB, soluble Fc $\gamma$ RIIB.

Table III. IgG levels in B cells (n=30,  $\mu$ g/ml, means  $\pm$  SD).

Group	IgG concentration
Control-Health	19.608 $\pm$ 4.838
sFc $\gamma$ RIIB-Health	6.054 $\pm$ 1.656 <sup>a</sup>
sFc $\gamma$ RIIB-ctDNA-Health	12.400 $\pm$ 1.803 <sup>a,b</sup>
Control-SLE	113.389 $\pm$ 6.768
sFc $\gamma$ RIIB-SLE	33.392 $\pm$ 1.521 <sup>c</sup>
sFc $\gamma$ RIIB-ctDNA-SLE	70.679 $\pm$ 6.595 <sup>d,e</sup>

<sup>a</sup>P<0.01 vs. Control-Healthy group; <sup>b</sup>P<0.05 vs. sFc $\gamma$ RIIB-Healthy group; <sup>c</sup>P<0.01 vs. Control-SLE group; <sup>d</sup>P<0.05 vs. Control-SLE group; <sup>e</sup>P<0.05 vs. sFc $\gamma$ RIIB-SLE group. SLE, systemic lupus erythematosus; sFc $\gamma$ RIIB, soluble Fc $\gamma$ RIIB.

group, while the relative expression of p-BTK/BTK in the virus-infected SLE and virus-infected healthy groups was significantly lower than that in the control SLE and control healthy groups following anti-ctDNA-IC stimulation (Fig. 3B and C). More importantly, the apoptotic rate of the B cells in the virus-infected SLE and healthy groups was respectively significantly higher than that in the control SLE and control healthy groups, and the apoptotic rate of the B cells in the anti-ctDNA-IC treatment group was higher than that in the ctDNA treatment group (Fig. 4A).

*sFc $\gamma$ RIIB and sFc $\gamma$ RIIB-IgG levels in serum of patients with SLE.* The levels of sFc $\gamma$ RIIB and sFc $\gamma$ RIIB-IgG in the serum of patients with SLE were lower than those in the serum of the healthy subjects. The level of sFc $\gamma$ RIIB-IgG in the patients with SLE was lower than that in the healthy subjects. No significant difference was observed between sFc $\gamma$ RIIB-IgG and sFc $\gamma$ RIIB in the serum of the healthy subjects (Table I).

*Effect of sFc $\gamma$ RIIB on human B cells.* Recombinant sFc $\gamma$ RIIB protein was successfully expressed and identified by western blot analysis. The results revealed that recombinant sFc $\gamma$ RIIB bound to immune complexes (ICs) in serum and reduced the secretion of IgG antibodies in B cells, suggesting that sFc $\gamma$ RIIB may inhibit the activation of B lymphocytes by combining with IC (Tables II and III). The relative expression levels of p-Lyn/Lyn p-DOK1/DOK1 and p-SHIP/SHIP in the SLE groups were lower, while the

relative expression of p-BTK/BTK was higher compared to the corresponding healthy groups. Furthermore, among the SLE groups, the relative expression levels of p-Lyn/Lyn, p-DOK1/DOK1 and p-SHIP/SHIP in the sFc $\gamma$ RIIB treatment subgroups were higher, while the relative expression of p-BTK/BTK was lower than that in the control subgroup (Fig. 4B and C).

*Effect of mFc $\gamma$ RIIB lentivirus on MRL/lpr SLE mice.* The mouse mFc $\gamma$ RIIB gene was successfully inserted into the TRE vector and packed into viruses. The titers of the expressed and regulated viruses were measured to reach 10<sup>6</sup> TU/ml. mFc $\gamma$ RIIB lentivirus and lentivirus regulatory plasmid were injected into the MRL/lpr SLE mice, and the effects were examined. As a result, in the prevention group and treatment group, mFc $\gamma$ RIIB lentivirus treatments significantly decreased urine albumin, serum anti-dsDNA antibody and serum anti-nuclear antibody levels, while increasing mFc $\gamma$ RIIB expression in spleen B cells (Fig. 5). In the prevention and treatment groups of B cells, the relative expression of p-BTK/BTK was increased, while the relative expression of p-SHIP/SHIP was decreased (Fig. 6). More importantly, the results of H&E staining revealed that in the MRL/lpr SLE mouse kidney tissue, a large number of lymphocytes infiltrated around the glomerulus and the glomerular capillaries became atrophied and hardened. In the liver tissue, mild histological alterations were observed, such as ballooning in the cytoplasm, dilatation in the central vein and hepatic sinusoids, and lymphocytic infiltrate in the hepatic lobules. In the lymph nodes, there were a large number of lymphocytes in the lymphoid follicles, the lymphoid nodules were enlarged, and the lymphoid follicles were proliferated. However, mFc $\gamma$ RIIB lentivirus treatments slightly ameliorated these pathologies, including decreased cytoplasmic swelling and lymphocyte infiltration (Fig. 7).

*Preventive and therapeutic effects of sFc $\gamma$ RIIB in MRL/lpr SLE mice.* Mouse sFc $\gamma$ RIIB gene was successfully cloned into the pET-sFc $\gamma$ RIIB plasmid, which was identified by DNA sequencing, and mouse recombinant sFc $\gamma$ RIIB protein was obtained by induction and was purified. Following treatment with mouse recombinant sFc $\gamma$ RIIB protein, some indexes in the MRL/lpr SLE mice were detected. As a result, in the prevention and treatment groups, in all sFc $\gamma$ RIIB protein treatments, the levels of sFc $\gamma$ RIIB and sFc $\gamma$ RIIB-IgG were significantly increased in a positive dose-dependent manner, while serum



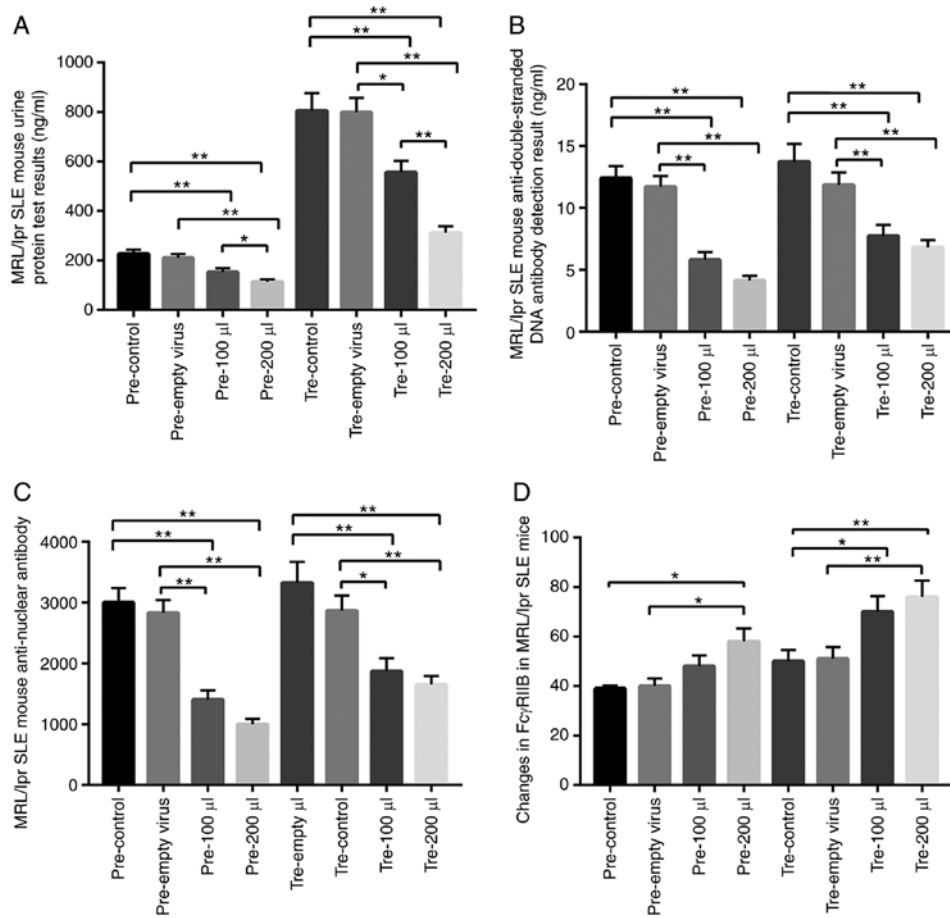


Figure 5. Target detection of MRL/lpr SLE mice following mFcγRIIB treatment. (A) Changes in urine protein levels. (B) Changes in serum anti-dsDNA antibody levels. (C) Changes in serum anti-nuclear antibody levels. (D) Changes in mFcγRIIB levels in B cells. pre-control, Control subgroup in the prevention group; pre-empty virus, empty virus subgroup in the prevention group; pre-100 μl, 100 μl mFcγRIIB lentivirus subgroup in the prevention group; pre-200 μl, 200 μl mFcγRIIB lentivirus subgroup in the prevention group; tre-control, control subgroup in the treatment group; tre-empty virus, empty virus subgroup in the treatment group; tre-100 μl, 100 μl mFcγRIIB lentivirus subgroup in the treatment group; tre-200 μl, 200 μl mFcγRIIB lentivirus subgroup in the treatment group. \*P<0.05; \*\*P<0.01; n=10 in each group. SLE, systemic lupus erythematosus; mFcγRIIB, membrane-bound type FcγRIIB; sFcγRIIB, soluble FcγRIIB.

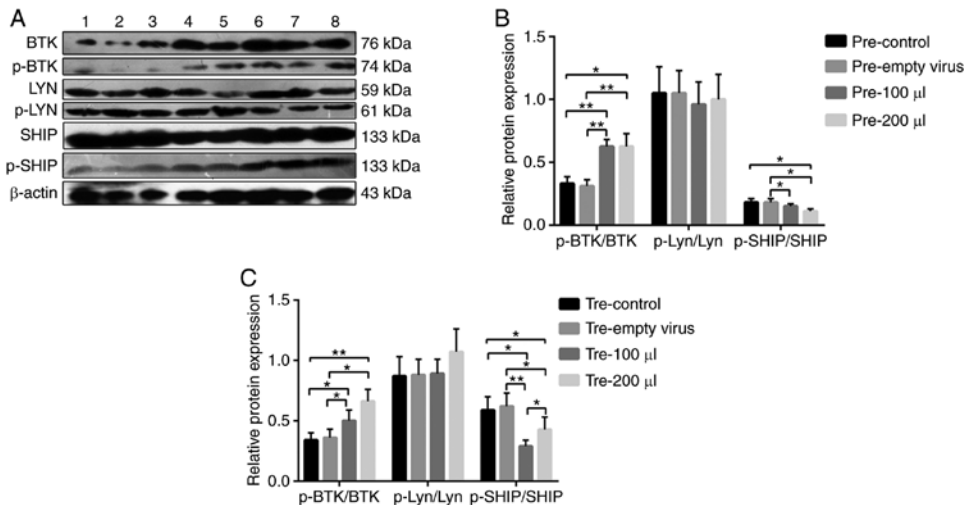


Figure 6. (A) The protein expression levels of BTK, p-BTK, Lyn, p-Lyn, SHIP and p-SHIP in MRL/lpr SLE mouse B cells were examined by western blot analysis, with β-actin as a loading control. (B and C) The phosphorylation and total protein levels of BTK, Lyn and SHIP were detected in B cells from MRL/lpr SLE mice after the infection of mFcγRIIB lentivirus, and the relative level for each phosphorylation-protein/each respective total protein was calculated. Lane 1: pre-empty virus, empty virus subgroup in the prevention group; lane 2: pre-control, control subgroup in the prevention group; lane 3: pre-100 μl, 100 μl mFcγRIIB lentivirus subgroup in the prevention group; lane 4: pre-200 μl, 200 μl mFcγRIIB lentivirus subgroup in the prevention group; lane 5: tre-control, control subgroup in the treatment group; lane 6: tre-empty virus, empty virus subgroup in the treatment group; lane 7: tre-100 μl, 100 μl mFcγRIIB lentivirus subgroup in the treatment group; lane 8: tre-200 μl, 200 μl mFcγRIIB lentivirus subgroup in the treatment group. \*P<0.05; \*\*P<0.01. Data are presented as means ± SD of 3 independent experiments. SLE, systemic lupus erythematosus; mFcγRIIB, membrane-bound type FcγRIIB; sFcγRIIB, soluble FcγRIIB; BTK, Bruton's tyrosine kinase; Lyn, Lyn proto-oncogene, Src family tyrosine kinase; DOK-1, docking protein 1; SHIP, inositol polyphosphate-5-phosphatase D.

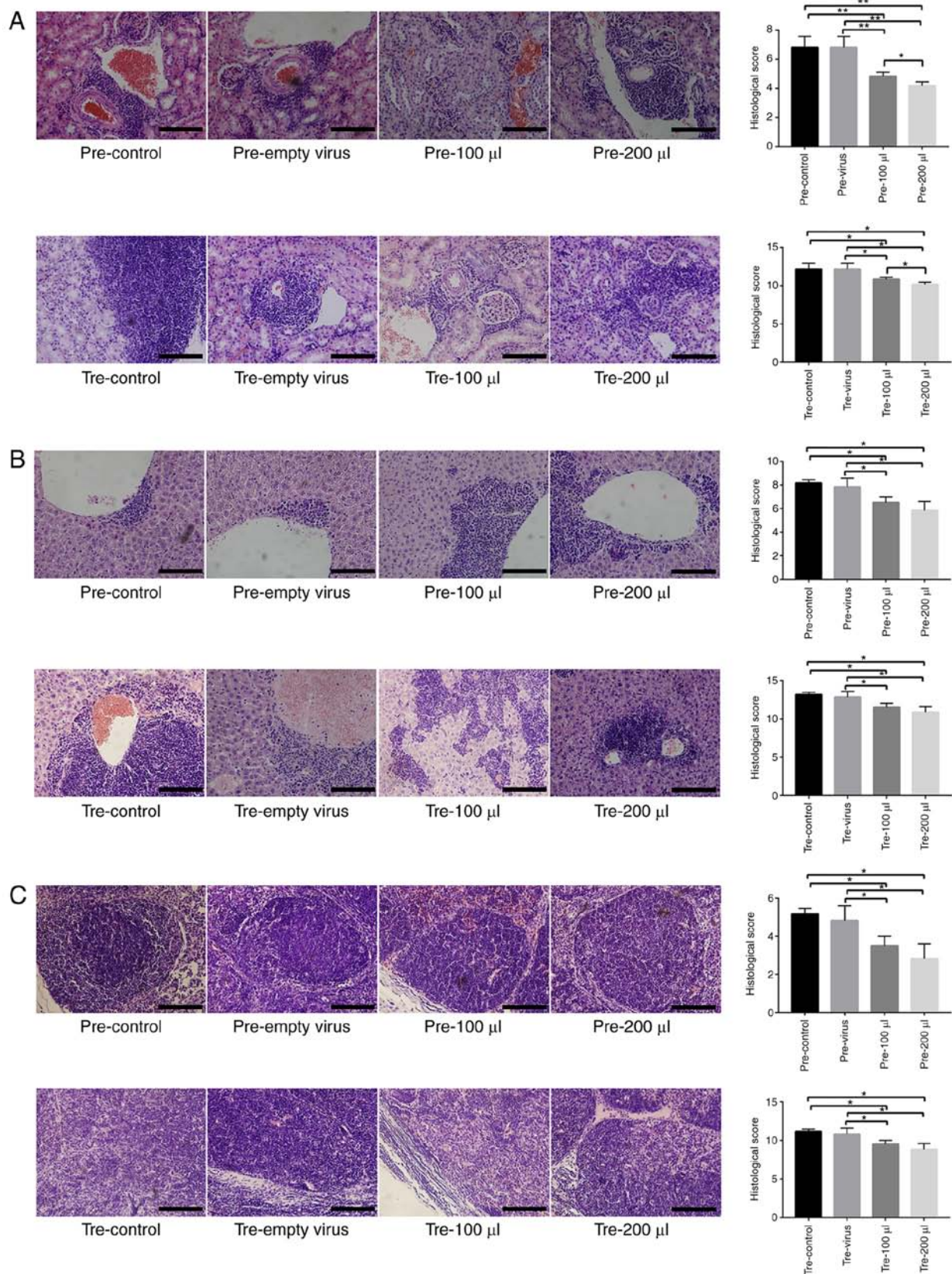


Figure 7. H&E staining results in mice. (A) Kidney tissue. (B) Liver tissue. (C) lymph gland. Representative images for HE results are shown. Scale bar, 25  $\mu$ m. \* $P$ <0.05; \*\* $P$ <0.01;  $n$ =10 in each group.

anti-dsDNA antibody and urine albumin levels were markedly decreased in a reverse dose-dependent manner (Fig. 8), as compared to the normal saline treatment. Moreover, the

relative expression levels of p-Lyn/Lyn and p-SHIP/SHP were increased, while the relative expression of p-BTK/BTK in B cells was decreased following sFc $\gamma$ RIIB protein treatment (Fig. 9).

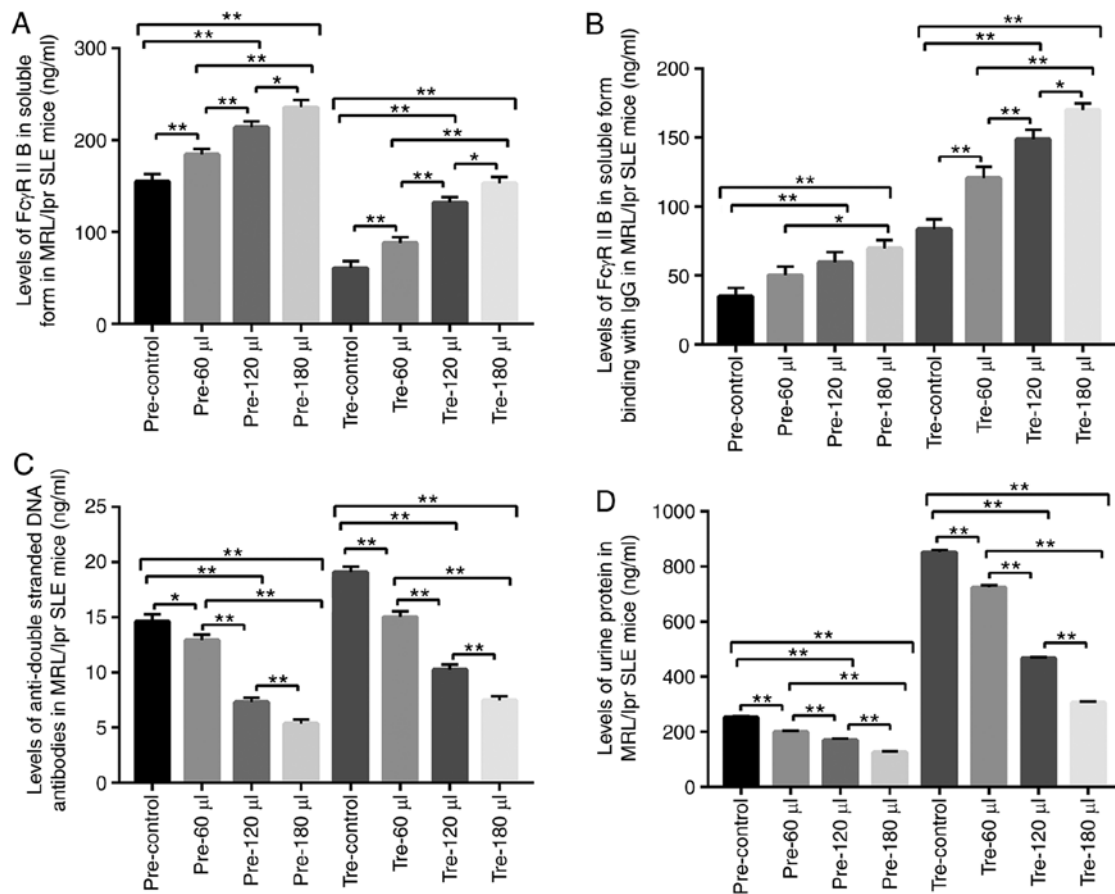


Figure 8. Target detection in MRL/lpr SLE mice. (A) Detection of sFcγRIIB. (B) Detection of FcγRIIB binding with IgG. (C) Detection of serum anti-double-stranded DNA antibody. (D) Detection of urine protein. pre-control, control subgroup in the prevention group; pre-60 μl, 4.8 μg sFcγRIIB subgroup in the prevention group; pre-120 μl, 9.6 μg sFcγRIIB subgroup in the prevention group; pre-180 μl, 14.4 μg sFcγRIIB subgroup in prevention group; tre-control, control subgroup in the treatment group; tre-60 μl, 4.8 μg sFcγRIIB subgroup in the treatment group; tre-120 μl, 9.6 μg sFcγRIIB subgroup in the treatment group; tre-180 μl, 14.4 μg sFcγRIIB subgroup in the treatment group. \*P<0.05; \*\*P<0.01; n=10 in each group. SLE, systemic lupus erythematosus; mFcγRIIB, membrane-bound type FcγRIIB; sFcγRIIB, soluble FcγRIIB.

## Discussion

FcγRIIB, an inhibitory receptor in the FcγR family (18), is composed of an extracellular domain containing two Ig-like structures and an intracellular region containing an ITIM motif (19,20). The extracellular region is an Fc region with a low affinity for binding all IgG subclasses and exists as a membrane-bound type and insoluble form. sFcγRIIB is produced by the hydrolysis of the mFcγRIIB extracellular region stimulated by antigens and cytokines or is produced by FcγRIIB gene splicing (21,22). In the present study, in order to examine the roles of mFcγRIIB and sFcγRIIB in SLE, patients with SLE and MRL/lpr SLE mouse models were utilized.

The serum of patients with SLE contains a large number of anti-nuclear antibodies and IgG type CICs (23), and research has indicated that FcγRIIB can be crosslinked to BCR or activated FcR by IC to inhibit the activation and antibody secretion of B cells (24,25). Therefore, in the present study, ctDNA and anti-ctDNA-IC were used to stimulate B lymphocytes from patients with SLE and healthy subjects following mFcγRIIB lentivirus transfection. It was found that ctDNA stimulation reduced B lymphocyte IgG antibody secretion following mFcγRIIB lentivirus

transfection, and exerted a more prominent effect on SLE B cells than on normal B cells. Furthermore, when the added IC reached a certain level, it directly inhibited the secretion of IgG antibody by B cells. Therefore, B cell-derived FcγRIIB is involved in preventing the *in vivo* production of autoreactive antibodies, providing a peripheral checkpoint for maintaining normal self-tolerance. The combination of FcγRIIB and IC provides an inhibitory feedback loop for B lymphocytes, thus maintaining the dynamic balance of antibody expression.

Following lentivirus vector transfection into MRL/lpr mice, the expression level of mFcγRIIB was increased in a dose-dependent manner with the lentiviral vector. In the presence of the DOX inducer, the transcriptional expression of the target gene was induced by the combining of expression product of regulatory plasmid with rtTA of the response plasmid. Therefore, the concentration of DOX inducer directly affects the transcription and expression levels of target genes (26). The levels of anti-nuclear antibodies, urinary albumin and anti-dsDNA in MRL/lpr mice were downregulated after the injection of virus containing Dox, due to the increase in mFcγRIIB which decreased the B cell secretion of antibodies. These results could deactivate signal transduction proteins by dephosphorylation to terminate BCR activation

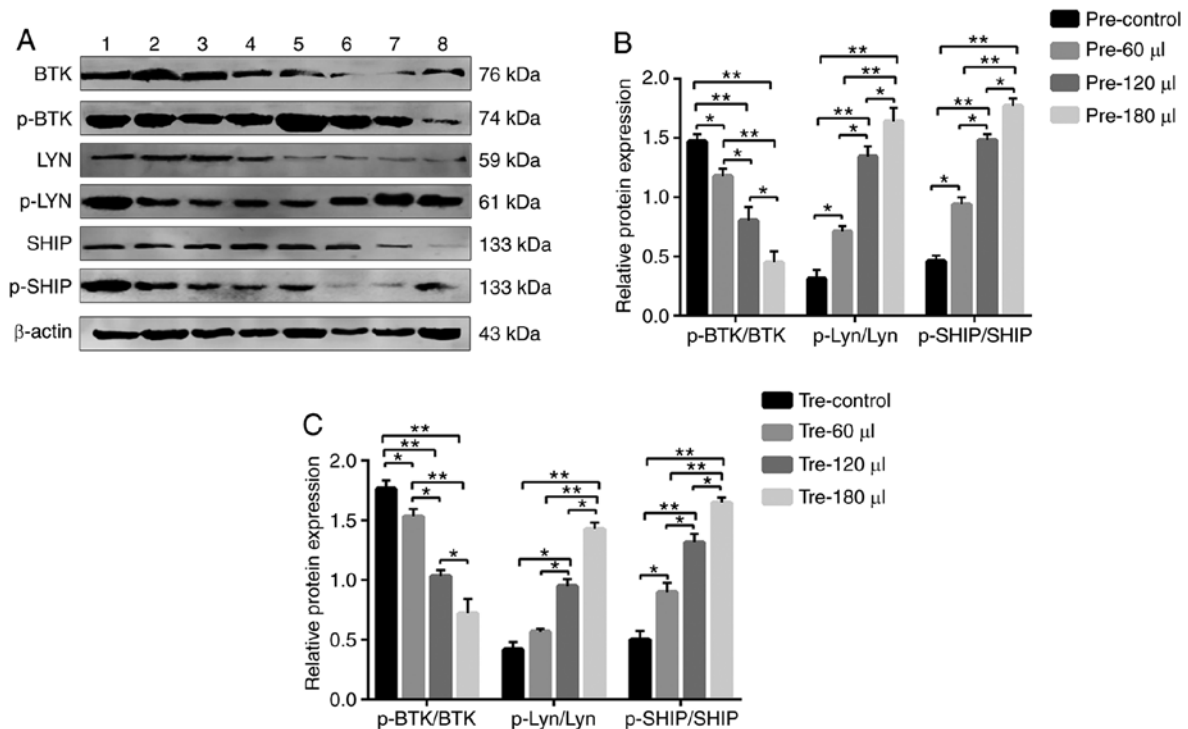


Figure 9. (A) The protein expression levels of BTK, p-BTK, Lyn, p-Lyn, SHIP and p-SHIP in MRL/lpr SLE mouse B cells were examined by western blot analysis, with  $\beta$ -actin as a loading control. (B and C) The phosphorylation and total protein levels of BTK, Lyn and SHIP were detected in B cells from MRL/lpr SLE mice after the infection of sFc $\gamma$ RIIB lentivirus, and the relative level for each phosphorylation-protein/each respective total protein was calculated. Lane 1: pre-control, control subgroup in the prevention group; lane 2: pre-60  $\mu$ l, 4.8  $\mu$ g sFc $\gamma$ RIIB subgroup in the prevention group; lane 3: pre-120  $\mu$ l, 9.6  $\mu$ g sFc $\gamma$ RIIB subgroup in the prevention group; lane 4: pre-180  $\mu$ l, 14.4  $\mu$ g sFc $\gamma$ RIIB subgroup in the prevention group; lane 5: tre-control, control subgroup in the treatment group; lane 6: tre-60  $\mu$ l, 4.8  $\mu$ g sFc $\gamma$ RIIB subgroup in the treatment group; lane 7: tre-120  $\mu$ l, 9.6  $\mu$ g sFc $\gamma$ RIIB subgroup in the treatment group; lane 8: tre-180  $\mu$ l, 14.4  $\mu$ g sFc $\gamma$ RIIB subgroup in the treatment group. \* $P$ <0.05; \*\* $P$ <0.01; n=10 in each group. SLE, systemic lupus erythematosus; mFc $\gamma$ RIIB, membrane-bound type Fc $\gamma$ RIIB; sFc $\gamma$ RIIB, soluble Fc $\gamma$ RIIB; BTK, Bruton's tyrosine kinase; Lyn, Lyn proto-oncogene, Src family tyrosine kinase; DOK-1, docking protein 1; SHIP, inositol polyphosphate-5-phosphatase D.

signal transduction, inhibiting the activation, proliferation, differentiation and antibody production of B cells (27).

The Fc $\gamma$ RIIB signaling pathway is closely related to IgG antibody secretion in B cells. It mainly inhibits cell activation and proliferation through two signaling pathways (28). Pauls and Marshall (29) and Wang *et al* (30) found that Fc $\gamma$ RIIB activated tyrosine kinase (Lyn) by crosslinking with BCR through IC, causing the tyrosine phosphorylation of ITIM to recruit molecules, such as SHIP (inositol phosphatase). SHIP acts on 3,4,5-phosphatidylinositol triphosphate to hydrolyze it to 3,4-phosphatidylinositol diphosphate. 3,4-Phosphatidylinositol diphosphate prevents PIP3 from recruiting BTK and phospholipase  $\gamma$ 2 (PLC $\gamma$ 2) onto cell membranes following dephosphorylation, thereby reducing the intracellular calcium levels, which finally inhibits cell activation involving related kinases to reduce antibody production. ITIM transduction can inhibit cell proliferation by the activation of DOK1 and MAP kinase instead of SHIP (29,30). High concentrations of Fc $\gamma$ RIIB lead to the direct apoptosis of B cells by crosslinking with BCR to increase the phosphorylation of Lyn and SHIP1, and the simultaneous phosphorylation of BTK, independent of the ITIM pathway.

Corneth *et al* found that the cytoplasmic regions of human and mouse Fc $\gamma$ RIIB proteins contained ITIM motifs (28). This highly conserved 13 amino acid sequence encoded by the C3 exon contains a common inhibitory sequence, I/VxYxL, which can prevent the ITIM motif from transmitting activation signaling

by cross-linking BCR, Fc $\gamma$ RI, and Fc $\gamma$ RIII. When Fc $\gamma$ RIIB crosslinks other activation receptors containing ITIM, ITIM can inhibit cell activation and proliferation by activating Lyn to recruit SHIP1 or by activating DOK1 without SHIP recruitment (28).

It has been reported that recombinant human sFc $\gamma$ RIIB inhibited SLE membrane-type IC-mediated tissue damage by interfering with the *in vitro* binding of IC to B cells (31,32). Recombinant human sFc $\gamma$ RIIB plays a role by competitively binding IgG sites with mFc $\gamma$ RIIB *in vivo*; however, the mechanisms responsible for this blocking effect have not been extensively investigated (33).

Recombinant human sFc $\gamma$ RIIB inhibits the *in vitro* secretion of IgG-type antibodies by B cells. However, the mechanisms involved remain unclear. In the present study, following the stimulation of B cells from patients with SLE with recombinant human sFc $\gamma$ RIIB to secrete IgG-type antibodies, BTK, Lyn, SHIP and DOK1 were detected downstream of the sFc $\gamma$ RIIB and BCR signal transduction pathways. As a result, the phosphorylation levels of Lyn, SHIP and DOK1 were increased, while the phosphorylation level of BTK was decreased, consistent with those mediated by mFc $\gamma$ RIIB signal transduction, which proved that recombinant human sFc $\gamma$ RIIB binds to mFc $\gamma$ RIIB by bridging IgG type anti-sFc $\gamma$ RIIB autoantibody, and then initiated a series of signal transduction pathways. Inhibitory signals produced by human sFc $\gamma$ RIIB antagonizes activation signals produced by BCR, which eventually leads to B cell inhibition.

Recombinant human sFc $\gamma$ RIIB has been shown to alleviate the symptoms of proteinuria and weight loss in NZB/NZW F1 SLE model mice induced by IC, and to improve the survival rate of model mice with prophylactic application (34). However, this previous study did not explore the detailed mechanisms of sFc $\gamma$ RIIB alleviating SLE. After injecting human sFc $\gamma$ RIIB into each group of model mice, it was observed that the serum sFc $\gamma$ RIIB levels in the prevention and treatment groups increased with the increased dose of injected sFc $\gamma$ RIIB, and the sFc $\gamma$ RIIB level in the prevention group was higher than that in the treatment group. Simultaneously, the titers of anti-dsDNA antibodies and the urinary protein in the 2 groups decreased. Recombinant human sFc $\gamma$ RIIB inhibited the *in vivo* B cell secretion of IgG antibody. Of note, it was found in the present study that the phosphorylation levels of Lyn and SHIP were increased significantly with an increase in the sFc $\gamma$ RIIB dose injected into SLE model mice, which may have inhibited the downstream function of ITIM signal regulation and the release of calcium ions through the BCR signal transduction pathway (35). The phosphorylation levels of BTK in the prevention and treatment groups were significantly decreased with the increase in exogenous sFc $\gamma$ RIIB, indicating that the phosphorylation of BTK was not blocked when sFc $\gamma$ RIIB was deficient, while the phosphorylation of BTK was inhibited when sFc $\gamma$ RIIB was restored or enhanced. Therefore, it was surmised that sFc $\gamma$ RIIB inhibited the activation of B cells by inhibiting the activation of BCR pathway.

In conclusion, the present study demonstrated that recombinant Fc $\gamma$ RIIB inhibited B cell IgG antibody secretion by altering the phosphorylation levels of downstream proteins involved in the Fc $\gamma$ RIIB signaling pathway. Simultaneously, the transduction of mFc $\gamma$ RIIB lentivirus into MRr/lpr SLE mice further improved the symptoms of SLE mice, suggesting that Fc $\gamma$ RIIB may play a role in improving the activation, proliferation and antibody secretion of B cells, providing a new approach and method for the prevention and treatment of SLE patients. However, further experiments are required to address the conclusion on how Fc $\gamma$ RIIB regulates the phosphorylation of downstream proteins of Fc $\gamma$ RIIB signaling pathway, suppresses B cell activation to ameliorate systemic lupus erythematosus, and promotes the apoptosis of B cells.

### Acknowledgements

Not applicable.

### Funding

The present study was funded by the Ningxia High School First-Class Disciplines (West China First-Class Disciplines Basic Medical Sciences at Ningxia Medical University, no. NXYLXK2017B07), the National Natural Science Foundation of China (no. 81160375) and the Ningxia Medical University Scientific Research Project (XY201725).

### Availability of data and materials

The datasets used and/or analyzed during the current study are available from the corresponding author upon reasonable request.

### Authors' contributions

LS and XC performed the experiments, analyzed the data and wrote the manuscript. SC, JW, HX and HL performed the experiments and collected the data. ZY conceived and designed the study, obtained the funding and revised the manuscript. All authors have read and approved the final manuscript.

### Ethics approval and consent to participate

The present study was approved the Ethics Committee of Ningxia Medical University. All subjects signed informed consent forms prior to their inclusion in the study. The animal experiments were approved by the Animal Ethics Committee of Ningxia Medical University.

### Patient consent for publication

Not applicable.

### Competing interests

The authors declare that they have no competing interests.

### References

1. Das CM, Bezerra MC, Braga FN, da Justa Feijão MR, Gois AC, Rebouças VC, de Carvalho TM, Carvalho LN and Ribeiro AM: Clinical and immunological aspects and outcome of a Brazilian cohort of 414 patients with systemic lupus erythematosus (SLE): Comparison between childhood-onset, adult-onset, and late-onset sle. *Lupus* 25: 355-363, 2016.
2. Pamuk ON, Balci MA, Donmez S and Tsokos GC: The incidence and prevalence of systemic lupus erythematosus in Thrace, 2003-2014: A 12-year epidemiological study. *Lupus* 25: 102-109, 2016.
3. Dema B and Charles N: Advances in mechanisms of systemic lupus erythematosus. *Discov Med* 17: 247-255, 2014.
4. Park MJ, Kwok SK, Lee SH, Kim EK, Park SH and Cho ML: Adipose tissue-derived mesenchymal stem cells induce expansion of interleukin-10-producing regulatory B cells and ameliorate autoimmunity in a murine model of systemic lupus erythematosus. *Cell Transplant* 24: 2367-2377, 2015.
5. Park MJ, Lee SH, Kim EK, Lee EJ, Park SH, Kwok SK and Cho ML: Myeloid-Derived suppressor cells induce the expansion of regulatory B cells and ameliorate autoimmunity in the sanroque mouse model of systemic lupus erythematosus. *Arthritis Rheumatol* 68: 2717-2727, 2016.
6. McGaha TL, Ma Z, Ravishankar B, Gabunia K, McMenamin M and Madaio MP: Heterologous protein incites abnormal plasma cell accumulation and autoimmunity in MRL-MpJ mice. *Autoimmunity* 45: 279-289, 2012.
7. Taher TE, Bystrom J, Ong VH, Isenberg DA, Renaudineau Y, Abraham DJ and Mageed RA: Intracellular B lymphocyte signaling and the regulation of humoral immunity and autoimmunity. *Clin Rev Allergy Immunol* 53: 237-264, 2017.
8. Sondermann P and Oosthuizen V: The structure of Fc receptor/Ig complexes: Considerations on stoichiometry and potential inhibitors. *Immunol Lett* 82: 51-56, 2002.
9. Xu L, Li G, Wang J, Fan Y, Wan Z, Zhang S, Shaheen S, Li J, Wang L, Yue C, *et al*: Through an ITIM-independent mechanism the Fc $\gamma$ RIIB blocks B cell activation by disrupting the colocalized microclustering of the B cell receptor and CD19. *J Immunol* 192: 5179-5191, 2014.
10. Pauls SD, Ray A, Hou S, Vaughan AT, Cragg MS and Marshall AJ: Fc $\gamma$ RIIB-Independent mechanisms controlling membrane localization of the inhibitory phosphatase SHIP in human B cells. *J Immunol* 197: 1587-1596, 2016.
11. Lesourne R, Bruhns P, Fridman WH and Daëron M: Insufficient phosphorylation prevents fc gamma RIIB from recruiting the SH2 domain-containing protein-tyrosine phosphatase SHP-1. *J Biol Chem* 276: 6327-6336, 2001.

12. Tackenberg B, Nimmerjahn F and Lunemann JD: Mechanisms of IVIG efficacy in chronic inflammatory demyelinating polyneuropathy. *J Clin Immunol* 30: S65-S69, 2010.
13. Chu SY, Yeter K, Kotha R, Pong E, Miranda Y, Phung S, Chen H, Lee SH, Leung I, Bonzon C, *et al*: Suppression of rheumatoid arthritis B cells by XmAb5871, an anti-CD19 antibody that coengages B cell antigen receptor complex and Fc $\gamma$  receptor IIB inhibitory receptor. *Arthritis Rheumatol* 66: 1153-1164, 2014.
14. Gesheva V, Kerekov N, Nikolova K, Mihaylova N, Todorov T, Nikolova M and Tchobanov A: Suppression of dsDNA-specific B lymphocytes reduces disease symptoms in SCID model of mouse lupus. *Autoimmunity* 47: 162-172, 2014.
15. Soni C, Domeier PP, Wong EB, Shwetank, Khan TN, Elias MJ, Schell SL, Lukacher AE, Cooper TK and Rahman ZS: Distinct and synergistic roles of Fc $\gamma$ RIIB deficiency and 129 strain-derived SLAM family proteins in the development of spontaneous germinal centers and autoimmunity. *J Autoimmun* 63: 31-46, 2015.
16. Alegria-Schaffer A, Lodge A and Vattem K: Performing and optimizing western blots with an emphasis on chemiluminescent detection. *Methods Enzymol* 463: 573-599, 2009.
17. Nossent HC and Rekvig OP: Is closer linkage between systemic lupus erythematosus and anti-double-stranded DNA antibodies a desirable and attainable goal? *Arthritis Res Ther* 7: 85-87, 2005.
18. Sondermann P: The Fc $\gamma$ R/IgG interaction as target for the treatment of autoimmune diseases. *J Clin Immunol* 36: 95-99, 2016.
19. Wang J, Li Z, Xu L, Yang H and Liu W: Transmembrane domain dependent inhibitory function of Fc $\gamma$ RIIB. *Protein Cell* 9: 1004-1012, 2018.
20. Roghanian A, Stopforth RJ, Dahal LN and Cragg MS: New revelations from an old receptor: Immunoregulatory functions of the inhibitory Fc gamma receptor, Fc $\gamma$ RIIB (CD32B). *J Leukoc Biol* 6: 1002, 2018.
21. Zhang L, Cao XQ and Yang ZW: Preparation and function of human soluble Fc $\gamma$ RIIB. *Xi Bao Yu Fen Zi Mian Yi Xue Za Zhi* 28: 952-925, 2012 (In Chinese).
22. Magnusson SE, Andren M, Nilsson KE, Sondermann P, Jacob U and Kleinau S: Amelioration of collagen-induced arthritis by human recombinant soluble Fc $\gamma$ RIIB. *Clin Immunol* 127: 225-233, 2008.
23. Magro-Checa C, Schaarenburg RA, Beart HJ, Huizinga TW, Steup-Beekman GM and Trouw LA: Complement levels and anti-C1q autoantibodies in patients with neuropsychiatric systemic lupus erythematosus. *Lupus* 25: 878-888, 2016.
24. Sun JB, Xiang Z, Smith KG and Holmgren J: Important role for Fc $\gamma$ RIIB on B lymphocytes for mucosal antigen-induced tolerance and Foxp3+ regulatory T cells. *J Immunol* 191: 4412-4422, 2013.
25. Daëron M and Lesourne R: Negative signaling in Fc receptor complexes. *Adv Immunol* 89: 39-86, 2006.
26. Wong KE, Mora MC, Skinner M, Page SM, Crisi GM, Arenas RB, Schneider SS and Emrick T: Evaluation of PolyMPC-dox prodrugs in a human ovarian tumor model. *Mol Pharm* 13: 1679-1687, 2016.
27. Vásquez A, Baena A, González LA, Restrepo M, Muñoz CH, Vanegas-García A, Ortiz-Reyes B, Abdoel N, Rojas M, García LF and Vásquez G: Altered recruitment of lyn, syk and ZAP-70 into lipid rafts of activated B cells in systemic lupus erythematosus. *Cell Signal* 58: 9-19, 2019.
28. Corneth OB, Wolternil RG and Hendriks RW: BTK signaling in B cell differentiation and autoimmunity. *Curr Top Microbiol Immunol* 393: 67-105, 2016.
29. Pauls SD and Marshall AJ: Regulation of immune cell signaling by SHIP1: A phosphatase, scaffold protein, and potential therapeutic target. *Eur J Immunol* 47: 932-945, 2017.
30. Wang Q, Vogan EM, Nocka LM, Rosen CE, Zorn JA, Harrison SC and Kuriyan J: Autoinhibition of bruton's tyrosine kinase (Btk) and activation by soluble inositol hexakisphosphate. *Elife* 4: e06074, 2015.
31. Akiyama M, Suzuki K, Yamaoka K, Yasuoka H, Takeshita M, Kaneko Y, Kondo H, Kassai Y, Miyazaki T, Morita R, *et al*: Number of circulating follicular helper 2 T cells correlates with IgG4 and interleukin-4 levels and plasmablast numbers in IgG4-related disease. *Arthritis Rheumatol* 67: 2476-2481, 2015.
32. Awe O, Hufford MM, Wu H, Pham D, Chang HC, Jabeen R, Dent AL and Kaplan MH: Expression in T follicular helper cells limits CD40L-dependent germinal center B cell development. *J Immunol* 195: 3705-3715, 2015.
33. Iwata S and Tanaka Y: The importance of B cell-T cell interaction in autoimmune diseases. *Nihon Rinsho Meneki Gakkai Kaishi* 38: 398-402, 2015 (In Japanese).
34. Zhang M, Yu G, Chan B, Pearson JT, Rathanaswami P, Delaney J, Lim AC, Babcook J, Hsu H and Gavin MA: Interleukin-21 receptor blockade inhibits secondary humoral responses and halts the progression of preestablished disease in the (NZB x NZW)F1 systemic lupus erythematosus model. *Arthritis Rheumatol* 67: 2723-2731, 2015.
35. Seda V and Mraz M: B-Cell receptor signalling and its cross-talk with other pathways in normal and malignant cells. *Eur J Haematol* 94: 193-205, 2015.



This work is licensed under a Creative Commons Attribution-NonCommercial-NoDerivatives 4.0 International (CC BY-NC-ND 4.0) License.